THE PROTEIN SOCIETY

Molecular dynamics of the P450cam–Pdx complex reveals complex stability and novel interface contacts

Scott A. Hollingsworth and Thomas L. Poulos*

Departments of Chemistry, Pharmaceutical Sciences, and Molecular Biology and Biochemistry, University of California, Irvine, California 92697

Received 26 August 2014; Accepted 5 October 2014
DOI: 10.1002/pro.2583
Published online 11 October 2014 proteinscience.org

Abstract: Cytochrome P450cam catalyzes the stereo and regiospecific hydroxylation of camphor to 5-*exo*-hydroxylcamphor. The two electrons for the oxidation of camphor are provided by putidaredoxin (Pdx), a Fe_2S_2 containing protein. Two recent crystal structures of the P450cam–Pdx complex, one solved with the aid of covalent cross-linking and one without, have provided a structural picture of the redox partner interaction. To study the stability of the complex structure and the minor differences between the recent crystal structures, a 100 nanosecond molecular dynamics (MD) simulation of the cross-linked structure, mutated *in silico* to wild type and the linker molecule removed, was performed. The complex was stable over the course of the simulation though conformational changes including the movement of the C helix of P450cam further toward Pdx allowed for the formation of a number of new contacts at the complex interface that remained stable throughout the simulation. While several minor crystal contacts were lost in the simulation, all major contacts that had been experimentally studied previously were maintained. The equilibrated MD structure contained a mixture of contacts resembling both the cross-linked and noncovalent structures and the newly identified interactions. Finally, the reformation of the P450cam Asp251–Arg186 ion pair in the MD simulation mirrors the ion pair observed in the more promiscuous CYP101D1 and suggests that the Asp251–Arg186 ion pair may be important.

Keywords: cytochrome p450; redox partner; molecular dynamics

Introduction

Cytochromes P450 (P450 or CYPs) are heme-containing protein monooxygenases that catalyze the oxidation of a wide range of organic compounds.[1,2] Prevalent in all kingdoms of life, there have been over 18,000 CYP genes identified with at least 57 CYP genes reported in humans.[2–4] While diverse in function and substrate specificity, P450 enzymes activate molecular dioxygen for the following generalized hydroxylation reaction:

$$R-H + O_2 + 2e^- + 2H^+ \rightarrow R-OH + H_2O$$

Due in no small part to their different specificities for substrates and reactions, P450s have been a large focus in the fields of pharmaceutical research, biosensor, and bioconversion among many others.[5–8]

P450cam (CYP101A1) from *Pseudomonas putida*, one of the most extensively characterized

Abbreviations: ET, electron transfer; MD, molecular dynamics; ns, nanosecond; Pdr, Putidaredoxin reductase; Pdx, Putidaredoxin; ps, picosecond.

Additional Supporting Information may be found in the online version of this article.

Grant sponsor: Institutional Chemical and Structural Biology Training Grant Predoctoral Fellowship; Grant number: T32-GM10856 (to S.A.H.); Grant sponsor: NIH; Grant number: GM57353 (to T.L.P.); Grant sponsor: XSEDE; Grant number: TG-MCB130001 (to S.A.H. and T.L.P.).

*Correspondence to: Thomas L. Poulos; Department of Molecular Biology and Biochemistry, University of California, Irvine, CA 92697-3900. E-mail: poulos@uci.edu

P450 enzymes in terms of structure and function, catalyzes the stereo- and regiospecific hydroxylation of camphor to 5-hydroycamphor.[9,10] Like almost all P450 enzymes, P450cam accepts electrons from a redox partner to initiate the hydroxylation reaction. In the P450cam system, electrons are shuttled from NADH by the flavin adenine dinucleotide (FAD)-containing putidaredoxin reductase (Pdr) to the Fe_2S_2-containing putidaredoxin (Pdx), which then delivers two electrons, one at a time, to P450cam.[9,11] Previous work has shown that Pdx plays an effector role upon binding to P450cam for the donation of the second electron that induces structural changes in P450cam.[11,12] In addition to the known structures of all three individual components of this relay pathway, the co-crystal structure of Pdr–Pdx has also been solved, leaving only one complex left unsolved in the P450cam electron transfer pathway.[13–17] Despite a great deal of effort, however, the P450cam-Pdx complex structure had remained elusive until recently.

In two recent and separate studies, the 3D structure of the P450cam–Pdx complex was solved through x-ray crystallography and NMR spectroscopy. Using covalent cross-linking chemistry, Tripathi *et al*.[18] were able to trap the complex through flexible linkers and select mutagenesis resulting in the first structure of P450cam–Pdx (henceforth referred to as the cross-linked structure). Immediately following this finding, Hiruma *et al*.[19] solved the complex structure without the use of covalent chemistry using only a series of mutations on both P450cam and Pdx (henceforth referred to as the noncovalent structure) in addition to the NMR structure. While solved independently and using different approaches, the complexes are the same. The crystal structures showed significant differences to the working computational models that had been developed previously, notably that Pdx rotated by 90 degrees from what had been predicted.[20] Both structures also revealed Pdx binding to the open form of P450cam, which is consistent with extensive previous studies.[20–24] However, there are several differences between the cross-linked and noncovalent structures at the important P450cam–Pdx interface. As the complex is believed to be dynamic, it is possible that these small differences could be hints at the dynamic nature of the interactions between P450cam and Pdx. As molecular dynamics (MD) has proven to be a useful tool in studying both P450 individually and in related redox pairs, this method could provide a great deal of insight into the newly solved structures.[15,25,26]

As each of these structures represents a snapshot of the possible complex trapped in a crystal, it is imperative to study this complex in a dynamic fashion to not only reveal what contacts remain in an equilibrated structure but if any new contacts emerge through simulation that may have been disallowed in the crystal. What we present in this study is such an analysis. We performed a 100 ns MD simulation of the P450cam–Pdx complex to study the complex's stability and interface. The resulting equilibrated structure revealed not only a hybrid complex of both crystal structures, but several new contacts not seen in either structure appear with small conformational arrangements that may represent previously unobserved important structural contacts. In addition, the reformation of the Arg186–Asp251 ion pair in the MD simulation, broken in all known structures of the complex, has led to a reevaluation of the electron density of the previously solved crystal structures with regards to the proton relay network.

Results

The crosslink free reduced P450cam–Pdx complex solved by Tripathi *et al*[18] was used as the starting point of the 100 ns simulation. Once the initial minimization restraints were removed from the system, both P450cam and Pdx remained both individually stable with few large scale conformational changes while the complex itself showed a remarkable degree of stability over the course of the simulation (Fig. 1). The changes in root-mean squared displacement (RMSD) [Fig. 1(A)] upon the beginning of the simulation were caused by minor conformational changes in the loop regions on both P450cam and Pdx with one notable exception. Helix C of P450cam was found to move toward Pdx by approximately 5 Å early in the simulation and remains stable in its new conformation throughout the simulation. Root mean squared fluctuation (RMSF) analysis of the Cα atoms of each protein reinforce the relative stability of each protein as shown in Figure 1(B,C), where the most dynamic portions of either P450cam or Pdx occur on loops far removed from either active site and the complex interface.

While the RMSD suggests that minor changes occurred in the complex structure, a structural overlay of both the cross-linked and noncovalent crystal structures with an equilibrated structure from the 100 nanosecond (ns) trajectory reveals several new changes in the structure [Fig. 1(D)]. Several of the loops of both P450cam and Pdx opposite from the helix C movement noted above have undergone changes to generate new contacts between the redox partners. In addition, Pdx has undergone a small rotation centered at a fulcrum of the iron–sulfur cluster. To monitor this rotation evolution, the dihedral formed by the C_α atoms of Pdx_{Val6} and Pdx_{Lys2} making up a stable β-strand away from the interface and two of the iron-coordinating nitrogen atoms of the P450cam heme was calculated over the simulation, which can be seen in Figure 2. As Pdx was shown to be stable through both RMSD and RMSF

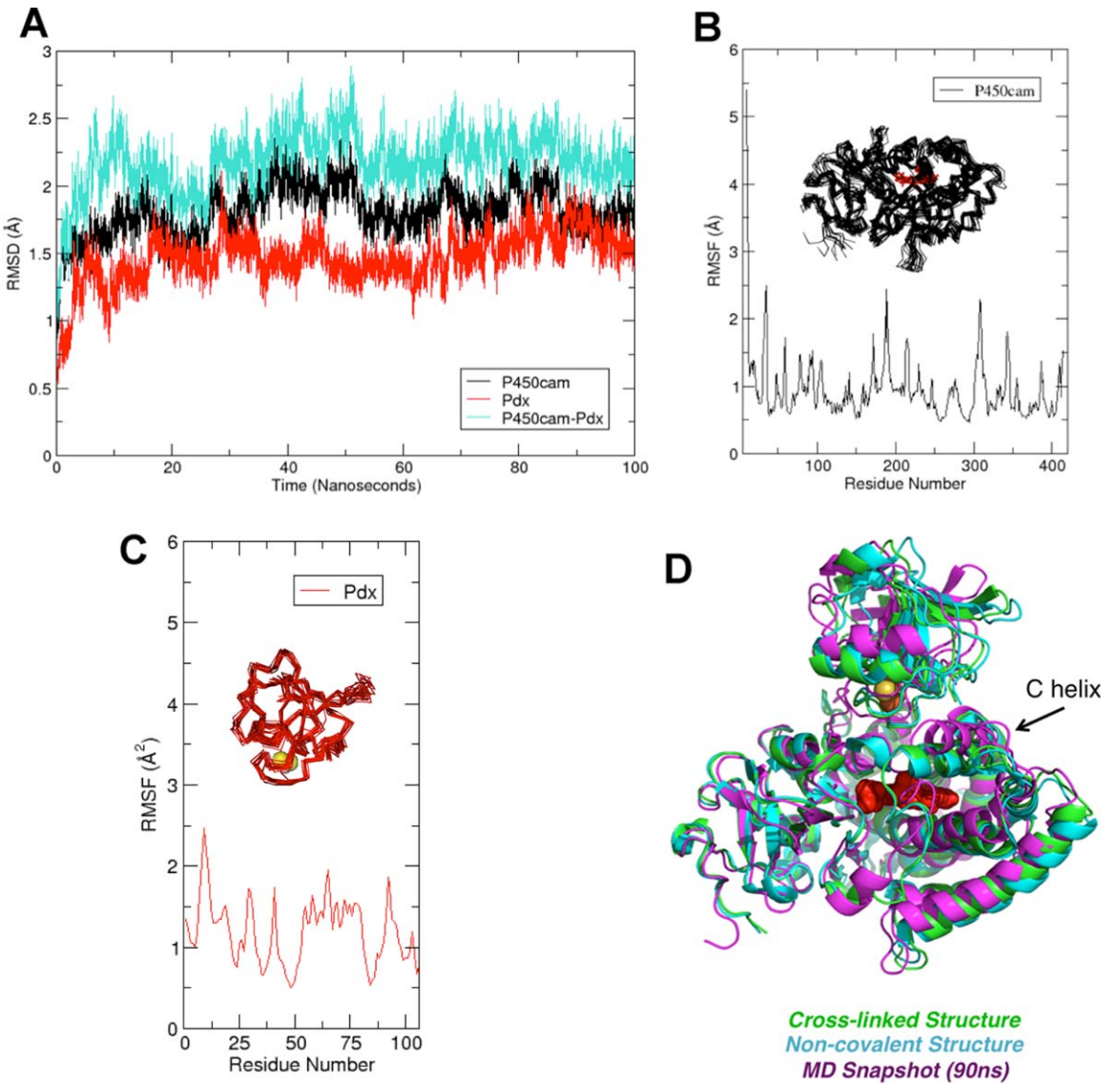

Figure 1. Stability of the P450cam–Pdx throughout the simulation. A) Shown are the RMSD evolutions for the backbone C_α atoms of P450cam (black), Pdx (Red), and the full P450cam–Pdx complex (Teal) throughout the course of the 100 nanosecond simulation. B) Calculated RMSF values for each C_α atom and an overlay of snapshots from every 10 ns throughout the simulation for both P450cam and C) Pdx. Both P450cam and Pdx show a high degree of stability individually and only minor changes as a complex. D) The three P450 structures, the cross-linked reduced of Tripathi *et al*.[18] (green), the noncovalent complex of Hiruma *et al*.[19] (Cyan), and a snapshot taken from near the end of the 100 ns simulation presented in this report (magenta) are overlaid by aligning all three along the backbone of P450cam. While the crystal structures overlap greatly, the MD structure shows significant differences in both helix C and a rotation of Pdx relative to P450cam in addition to small conformational changes in loops at the P450cam–Pdx interface.

analysis, the beta strand was chosen to study the Pdx rotation. The resulting Pdx orientation began near a value of -66° before equilibrating near 40 ns to a value near -56°, resulting in a 10 degree rotation of Pdx in relation to the heme group of P450cam. The mean distance from the iron–sulfur cluster to the heme iron over the final 25 ns was found to be 16.05 ± 0.27 Å (one sigma), showing good agreement with both the cross-linked (16.1 Å) and noncovalent (16.3 Å) crystal structures demonstrating that this rotation does not affect the heme-to-cluster distance.

As the interface between P450cam and Pdx is of great importance, time averaged contacts defined by a distance cutoff of 3.5 Å between nonhydrogen atoms averaged over time of the simulation were calculated over the final 25 ns of the simulation and over the full simulation to be directly compared to those observed in both the cross-linked and noncovalent structures. This analysis over the final equilibrated 25 ns is shown in Table I by summing all contacts made between any given pair of residues. Of the top time averaged contacts, only six and four of the contacts had been observed in the noncovalent

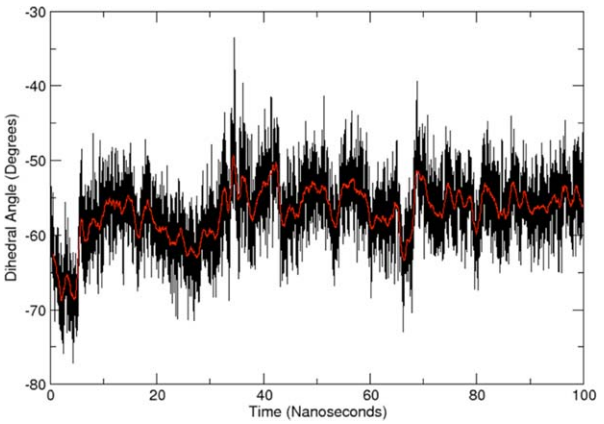

Figure 2. Rotation of Pdx in relation to P450cam. Pdx undergoes a small rotation with a fulcrum at the Fe_2S_2 cluster, monitored by calculated the dihedral angle formed by the NA and NC atoms of the P450cam heme and the C_α atoms of V6 and K2 of the central β-strand of a three stranded β-sheet of Pdx, which was fairly stable through the simulation, causing it to be chosen to study the movement of Pdx relative to the heme.

and cross-linked structures, respectively with an additional nine novel contacts. Further analysis of the contacts observed in either the cross-linked or noncovalent structures revealed that a number of contacts were broken early in the simulation and replaced by a host of new contact pairs, which are summarized by Table II and in more detail in Supporting Information Table SI.

Focusing on the contacts that had been previously described by the two crystal structures, the final MD structure resembles a cross between both the cross-linked and noncovalent structures. The salt-bridge of $P450cam_{Arg112}$ and Pdx_{Asp38} is especially important in the second electron transfer step, reduction of the oxy-complex to generate Compound I that then hydroxylates the substrate.[11,27,28] Other major electrostatic interactions observed in both structures, however, are weakened in the MD structure when compared to either crystal structure. The $P450cam_{Glu76}$–Pdx_{Arg66} interaction[11,18] observed in both structures is broken quickly in the MD structure and never regained, equilibrating at a distance nearly double that of either crystal distance. The third electrostatic interaction between $P450cam_{Asp125}$–Pdx_{Tyr33}[11,19] is weakened from what was seen in the cross-linked structure and closely resembles the noncovalent structure at the end of the simulation. The final three contact pairs previously described, which all include $P450cam_{Trp106}$, serve to further reinforce the importance of that residue in partner binding and activity.[11,29] The interfacial hydrogen bond that was observed in the cross-linked structure, $P450cam_{Asn116}$–Pdx_{Trp106}, was conserved throughout the full simulation. Finally, the major van der Waals interactions from the cross-linked structure such as $P450cam_{Ala113}$–Pdx_{Trp106} and $P450cam_{Arg109}$–Pdx_{Trp106} more closely resemble the cross-linked structure after equilibration and 100 ns of simulation.

In addition to the small number of contacts that had been previously described in the crystal structure, there were a number of new contacts that were formed in the simulation (Fig. 3). The strongest of these new interactions was a newly formed hydrogen bond between $P450cam_{Glu76}$ and Pdx_{Ser42} highlighted in Figure 3(A). This contact was formed owing to a conformational change on a loop of Pdx that occurred within the first 5 ns of the simulation. The interaction is dynamic as it switches between a single and bifurcated hydrogen bond throughout the simulation. A similar rearrangement on a Pdx-facing surface exposed loop of P450cam and a corresponding Pdx loop resulted in the formation of two additional hydrogen bonds between $P450cam_{Val345}$–Pdx_{Gln25} and $P450cam_{Gln343}$–Pdx_{Ala18} shown in Figure 3(B). These interactions are significant as in both crystal structures the corresponding distances between these contact pairs were 9.65 and 14.35 Å, respectively. This rearrangement represents the largest change at the P450cam–Pdx interface in the MD structure. Finally, a change in the iron–sulfur cluster coordinating loop of Pdx allowed for $P450cam_{Gly353}$ to a hydrogen bond to either Pdx_{Gly40} or Pdx_{Gly41} though a bifurcated hydrogen bond with both residues was never observed (Supporting Information Fig. S2). However, unlike the hydrogen bonds described previously, this interaction could also be characterized as a van der Waal interaction with a transient hydrogen bond that is closely connected to the van der Waal interaction of $P450cam_{His352}$–Pdx_{Gly40}, which is also highlighted in Supporting Information Figure S2.

Table I. *Top Time Averages Contact Pairs Over the Final 25 Nanoseconds*

P450cam residue	Pdx residue	Time averaged contact pairs	Previously documented[a]
Glu76	Ser42	3.59	
Arg109	Cys45	2.9396	CL
Val345	Gln25	2.39	
Arg112	Asp38	2.3604	CL, NC
Gln360	Asp38	2.11	
Arg109	Trp106	1.7171	CL, NC
Asn116	Trp106	1.6392	CL, NC
His352	Gly40	1.4621	
Arg109	Gln105	1.4154	CL
Lys344	Gly20	1.3913	
Ala113	Trp106	1.3179	CL, NC
Gly353	Gly41	1.2992	
Gln343	Ala18	1.2017	
Gly353	Gly40	1.0825	
Gln343	Val17	1.0096	

[a] CL, cross-linked structure (4JX1); NC, noncovalent structure (3W9C).

Table II. *Selected Comparisons of the Interactions at the Interface of P450cam and Pdx*

P450cam residue	P450cam atom	Pdx residue	Pdx atom	Cross-linked distance (Å)[a]	Noncovalent distance (Å)[a]	MD distance and σ of final 25 ns (Å)[b]
Glu76	OE1	Ser42	OG	5.8	7.0	**3.43 (0.81)**
Glu76	O	Arg66	NH1	2.8	2.9	**6.60 (1.85)**
Arg109	NH2	Cys45	O	**3.0**	6.3	2.89 (0.15)
Arg109	NH2	Thr47	CG2	**3.3**	9.5	3.52 (0.24)
Arg109	NH2	Gln105	O	**3.0**	9.8	2.88 (0.13)
Arg109	NH1	Trp106	OXT	4.8	9.6	**3.70 (0.98)**
Arg112	NH2	Asp38	OD2	**3.0**	3.4	2.88 (0.22)
Arg112	NH2	Asp38	CG	3.3	**3.8**	3.86 (0.27)
Ala113	CB	Trp106	CE3	**3.5**	**3.6**	3.55 (0.18)
Asn116	OD1	Trp106	NE1	**3.1**	5.0	3.28 (0.43)
Asp125	OD2	Tyr33	CZ	3.5	**5.5**	5.40 (0.71)
Asp125	CB	Tyr33	OH	3.5	3.2	**4.33 (0.72)**
Gln343	OE1	Ala18	N	15.3	13.4	**3.14 (0.49)**
Val345	O	Gln25	NE2	8.1	11.2	**3.17 (0.42)**
His352	CE1	Gly40	O	6.6	7.0	**3.34 (0.49)**
Gly353	O	Cys39	O	3.6	**4.3**	4.56 (0.31)
Gly353	CA	Ser42	OG	3.5	4.0	**8.28 (0.55)**
Gly353	O	Gly40	N	5.6	6.2	**3.23 (0.32)**
Gly353	O	Gly41	N	6.7	7.0	**3.24 (0.49)**
Leu356	CB	Cys39	O	3.4	3.5	**7.52 (0.20)**
Gln360	NE2	Asp38	OD1	6.7	8.2	**3.50 (0.68)**

[a] Distances in bold agree with the MD structure.
[b] Distances in bold are new contacts unique to the MD structure.

Two of the newly identified contacts surprisingly interact with the P450cam$_{Arg112}$–Pdx$_{Asp38}$ salt bridge that has been previously identified to be important. While the salt bridge remains one of the strongest contacts in the MD simulation, P450cam$_{Gln360}$ and P450cam$_{His361}$ interact with Pdx$_{Asp38}$ as well [Fig. 3(C)]. The first interaction of the two is created due to the breaking of the van der Waals interaction between P450cam$_{Gln360}$ and Pdx$_{Gly40}$ that was observed in the noncovalent structure in favor for the interaction of the polar glutamine with the negatively charged aspartic acid of Pdx. After the formation of this new interaction that supplements the previously described salt-bridge, P450cam$_{His361}$ begins to transiently hydrogen bond with the side chain of Pdx$_{Asp38}$ (Supporting Information Fig. S1). However, despite both of these new interactions with Asp38, the original salt bridge remains one of the strongest contact pairs in the complex.

In addition, one contact that had been previously observed in both crystal structures, P450cam$_{Arg109}$–Pdx$_{Trp106}$, was significantly strengthened due to the movement of P450cam helix C toward Pdx as was described previously [Fig. 3(D)]. While a movement of helix C toward Pdx was observed in both crystal structures, the movement of helix C toward Pdx continues further toward Pdx in the MD simulation. Through the movement of helix C, P450cam$_{Arg109}$ is able to reorient toward Pdx$_{Trp106}$ and allow for the formation of a transient hydrogen bond interaction in addition to the van der Waals interactions that had been previously described.

While each protein remained stable throughout the simulation within P450cam itself, the environment surrounding the essential Asp251, which participates in the proton relay network,[30] undergoes a possibly important change. Upon the beginning of the simulation, the Asp251–Arg186 ion pair that breaks in the crystal structure was reformed and remained in contact for the majority of the simulation though it was again temporarily broken twice before reforming (Supporting Information Fig. S3). However, the second ion pair of Asp251–Lys178 that was broken in each crystal structure remained broken throughout the simulation. These observations prompted us to re-examine the electron density map obtained from the refined covalent complex. There are four molecules in the asymmetric unit and in two of these the side chain of Arg186 is not visible while in a third asymmetric unit weak density indicates that Arg186 extends toward the surface away from Asp251. However, in the fourth asymmetric unit the 2Fo-Fc electron density map showed that Arg186 possibly adopts two orientations, one toward the surface and one near Asp251. We therefore performed a few rounds of refinement with Arg186 placed in multiple orientations and the resulting map clearly shows that Arg186 interacts with Asp251 similar to the MD structure (Fig. 4). It thus appears that even in the open conformation, the Asp251–Arg186 interaction is present but weakened relatively to the closed conformation.

Discussion

The recent structures of the P450cam–Pdx complex represent one last missing piece in the P450 electron

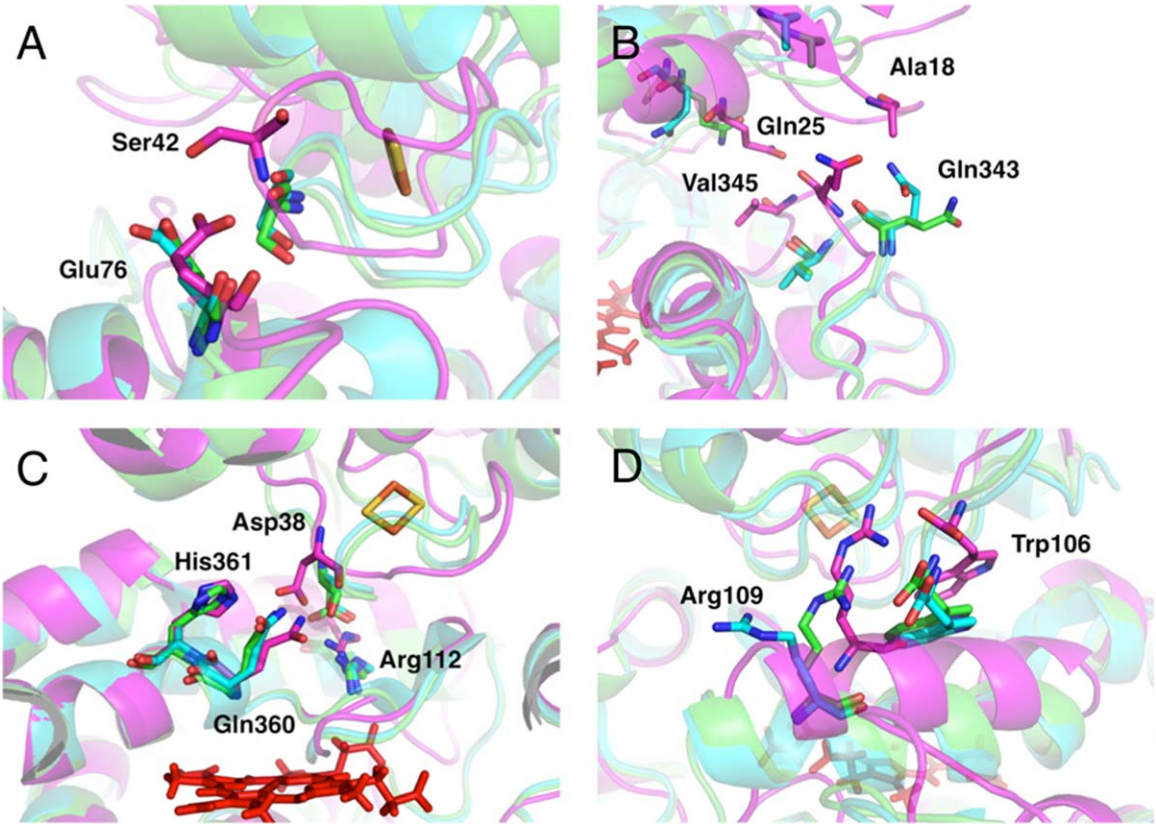

Figure 3. New contacts formed in the P450cam–Pdx complex. Shown are several of the new contacts that were formed in the P450cam–Pdx complex that were not observed in either of the published crystal structures. In all figures, the cross-linked structure is shown in green, noncovalent structure in cyan, and the final MD structure in magenta. A) Conformational changes in a Pdx interface loop allow for the formation of an interaction between $P450cam_{Glu76}$ and Pdx_{Ser42} that exists as either a single or bifurcated hydrogen bond. B) Loop rearrangements on both P450cam and Pdx allow for the formation of a pair of new hydrogen bonds; $P450cam_{Gln343}$–Pdx_{Ala18} and $P450cam_{Val345}$–Pdx_{Gln25}. C) Two P450 neighboring residues interact with the previously identified important intermolecular salt bridge of $P450cam_{Arg112}$ and Pdx_{Asp38}. The new interactions are caused when Pdx_{Asp38} rotates away from its salt bridge partner. The original salt bridge remains a strong interaction despite the addition of two additional interacting residues. D) Helix C of P450cam moves closer to Pdx than what was observed in either crystal structure to allow for a stronger interaction between $P450cam_{Arg109}$ and Pdx_{Trp106}.

transfer puzzle, although several questions remain unanswered. The crystal structures represent a single snapshot in time of the complex and the two crystal structures do show some differences in relation to the complex interface. In addition, dynamics clearly are important since the Pdx induced shift of P450cam from the closed to open conformation is closely tied to arming the proton coupled electron transfer machinery required for O_2 activation. Since structural changes are so intimately tied to the activation process, MD simulations can provide important insights into functional important structural changes.

The complex is stable throughout the 100 ns simulation. The most important change is that the C helix of P450cam, which has been previously identified as important to partner recognition, undergoes a conformational change that moves it closer to Pdx than what was observed in the complex crystal structures.[18,19,29] This emphasizes the importance of the C helix as this movement brings P450cam into closer proximity to Pdx and strengthens the intermolecular interactions that had previously been observed as the largest singular conformational change observed in the simulation. This movement of the C helix tightens the interactions with Pdx_{Trp106}, a residue known to be essential for activity.[11,29] In addition, Pdx undergoes a small rotation in relation to P450cam that allows for the formation of several new interactions between the redox partners and an enlargement of the interface. Despite several minor contacts that had been observed in the crystal structure being broken by these changes, the formation of a host of new contacts keeps the overall complex stable. When the top contacts from the MD simulation are used to describe the P450cam-Pdx interface, a striking observation emerges. Contacts that were observed in both crystal structures represent only a small number of contacts localized between only the intermolecular salt bridge and P450cam helix C while the new contacts make up the remainder of the interface (Fig. 5). In

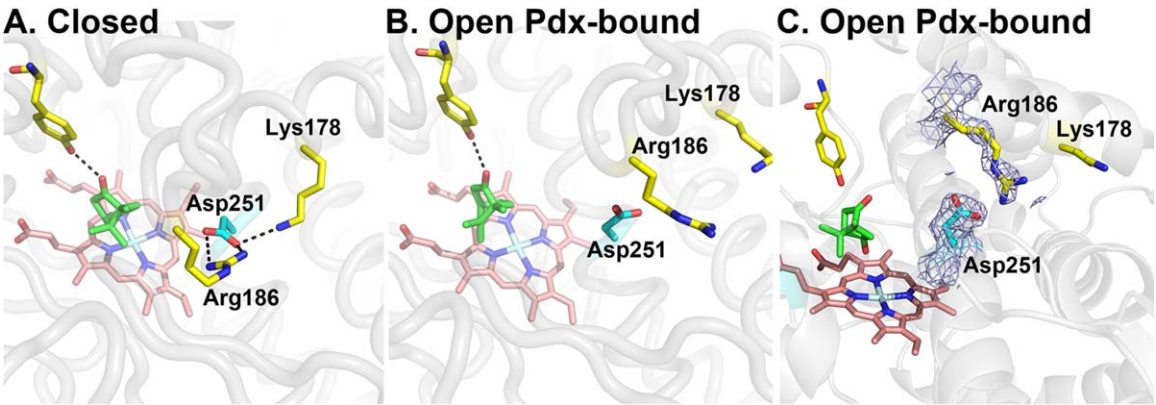

Figure 4. The Arg186–Asp251 ion pair is weakened but present in the open Pdx-bound complex. Panels A and B shows the environment of Asp251 in the closed and open structures as initially observed by Tripathi *et al*.[18] A re-examination of the electron density map, however, reveals that in one of the four P450cam molecules in the asymmetric unit Arg186 interacts with Asp251 (Panel C). The map shown is a 2Fo-Fc map contoured at 0.8σ while the density breaks up at 1.0σ. This indicates a relatively high mobility of Arg186 further suggesting that the Asp251–Arg186 interaction is not as strong as in the closed conformation.

the MD simulations, these large surfaces of Pdx and P450cam relax to each other increasing the interface surface significantly through small conformational changes and a small rotation of Pdx in relation to P450cam. These movements significantly increase the intermolecular contacts in the complex.

An important question to address is why these contacts were not observed in either crystal structure. The complex in the cross-linked structure will have its conformational freedom restricted by the covalent linkage and, in fact, several of the new contacts would be directly inhibited by the presence of these molecules. The initial cross-linked structure presented by Tripathi *et al*.[18] would restrict conformational freedom near the $P450cam_{Glu76}$–Pdx_{Ser42} and $P450cam_{Gly353}$–$Pdx_{Gly40/41}$ hydrogen bonds while the second cross linked structure would directly inhibit the formation of the hydrogen bond between $P450cam_{Val345}$ and Pdx_{Gln25} due to the presence of the cross-link site at the neighboring $P450cam_{Lys344}$ residue. Although the noncovalent crystal structure does not have these restrictions, in both crystal forms, Pdx is tightly packed with not just its P450cam redox partner but other P450 molecules in the crystal lattice. While what is observed in the crystal structure likely represents the lowest energy complex, the energy well in such electron transfer complexes is shallow in order to maintain rapid off-rates required for high turnover. MD thus provides a clearer picture on states that are nearly isoenergetic with the lowest free energy state.

An important hypothesis to have emerged from the P450cam–Pdx structure is the role of the essential Asp251 (Fig. 4). The Asp251Asn mutant dramatically lowers activity[30] and what little activity is left exhibits a large increase in the kinetic solvent isotope effect.[31] This suggests that Asp251 plays an important role in the delivery of protons to the iron-linked O_2 molecule that is essential for cleaving the O—O bond. However, in the closed P450cam structure Asp251 is ion paired with Arg186 and Lys178, which is totally inconsistent with its proposed role as a proton shuttling residue. When Pdx binds and the active site opens up, the Asp251 ion pairs are

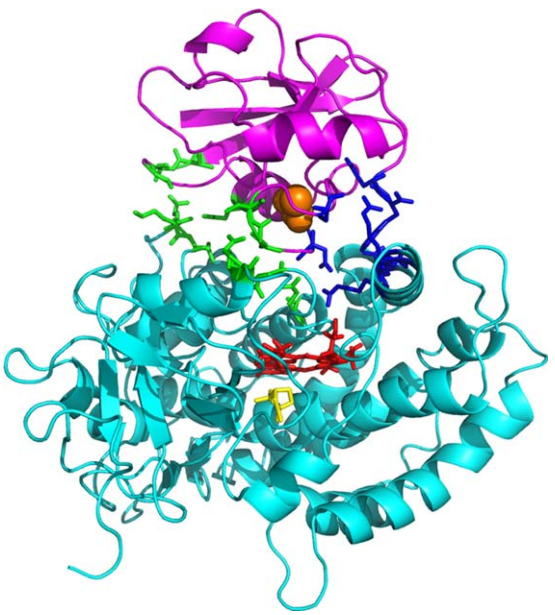

Figure 5. Major contacts observed in the P450cam–Pdx complex. Snapshot from the equilibrated P450cam (cyan)–Pdx (magenta) complex. The iron–sulfur cluster, heme, and camphor are shown in orange, red, and yellow for reference. While several of the major contacts observed in both crystal structures are conserved throughout the MD simulation (shown as blue sticks), the newly formed contacts in the MD simulation all occupy a different part of the P450cam–Pdx interface where minimal contacts were observed structurally. The residue contact pairs are taken from Table I. Recent experimental work has shown that contacts in this new region however may still play a role in partner recognition.

broken thus freeing Asp251 to serve its proposed role in proton transfer. The MD simulation, however, shows that the Asp251–Arg186 ion pair reforms for much of the simulation unlike the Asp251–Lys178 ion pair that is never reformed, which is supported by our re-examination of the electron density maps. This is particularly relevant in light of recent studies on a close homolog of P450cam and CYP101D1.[32] CYP101D1 catalyzes exactly the same reaction as P450cam, at the same rate, and uses a similar Pdx-like ferredoxin called Arx. In CYP101D1 its Asp251 homolog is also essential for activity but this Asp is ion paired with an Arg while the residue analogous to Lys178 in P450cam is Gly180 in CYP101D1. CYP101D1 is quite promiscuous with respect to redox partner since Pdx can support CYP101D1 camphor hydroxylation while the CYP101D1 redox partners exhibit no activity with P450cam.[32] This clearly means that CYP101D1 does not require the assistance of specific redox partner binding to activate the proton coupled electron transfer process likely because it's catalytically critical Asp259 has only one ion pair with an Arg residue and thus can more readily serve in a proton relay network without a large conformational adjustment. Our MD structure of the P450cam–Pdx complex with the Asp–Arg ion pair reforming thus closely resembles the ion pairing in CYP101D1. This further suggests that the Asp251-Arg186 pair might be important in the open conformation. These observations can be readily tested by suitably designed mutagenesis experiments.

Materials and Methods

The ferric P450cam–Pdx complex as solved by Tripathi *et al*.[18] was used as the starting point of the simulation. The covalent cross-linker molecules were removed and the cross-links sites mutated back to their wild type counterparts (Pdx_{Asp19} and $P450cam_{Lys344}$). The system was then placed in an octahedral unit cell with an angle of 109.47 degrees and solvated with 11,811 water molecules and neutralized through the addition of sodium ions. The full system consisted of a total 43,495 atoms. The Amber 12.0 suite (http://ambermd.org/) was used for all calculations.[33] The ff10 forcefield provided with the Amber 12.0 package was used for the protein, while the heme–Cys ligand parameters were taken from Shahrokh *et al*.[34] Parameters for the camphor were derived with antechamber and the gaff forcefield[35] using the BCC charging scheme.[36,37] Partial charges and optimal geometry for the Pdx iron–sulfur cluster were obtained using density functional theory and the 6-31G* basis set as implemented in Jaguar (Schrodinger) while average bond distances and angles were taken from the refined Pdx structure. The P450cam–Pdx crystal structure including crystallographic identified waters was solvated with box of TIP3 waters using 10 Å cushion. Counterions were added to maintain a net neutral charge.

The structure was prepared for production MD runs by first energy minimization for 1000 cycles with all heavy atoms except water molecules fixed in position followed by another 1000 cycles where all atoms were allowed to move. Production runs were performed with a 1 fs time step and coordinates saved every 10 ps. Temperature and pressure were held constant through weak coupling with a 1 ps pressure relaxation time and Langevin dynamics using a collision frequency of 1 ps^{-1}. Periodic boundary conditions were used with a particle-mesh Ewald implementation of the Ewald sum for the description of long-range electrostatic interactions.[38] A spherical cutoff of 10.0 Å was used for non-bonded interactions. Bonds involving hydrogen atoms were constrained using SETTLE.[39] Analysis was performed by using the Amber software suite, visual molecular dynamics, and locally developed analysis tools.[40,41]

Acknowledgments

The authors acknowledge Dr. Douglas Tobias for thoughtful discussions.

References

1. Poulos TL (2005) Structural biology of heme monooxygenases. Biochem Biophys Res Commun 338:337–345.
2. Poulos TL (2014) Heme enzyme structure and function. Chem Rev 114:3919–3962.
3. Nelson DR (2009) The cytochrome p450 homepage. Hum Genomics 4:59–65.
4. Strushkevich N, MacKenzie F, Cherkesova T, Grabovec I, Usanov S, Park HW (2011) Structural basis for pregnenolone biosynthesis by the mitochondrial monooxygenase system. Proc Natl Acad Sci USA 108:10139–10143.
5. Ortiz de Montellano PR (2005) Cytochrome P450: structure, mechanism, and biochemistry. New York: Kluwer Academic/Plenum Publishers.
6. Bistolas N, Wollenberger U, Jung C, Scheller FW (2005) Cytochrome P450 biosensors - a review. Biosens Bioelectron 20:2408–2423.
7. Guengerich FP (1999) Cytochrome P-450 3A4: regulation and role in drug metabolism. Ann Rev Pharmacol Toxicol 39:1–17.
8. Rendic S, Guengerich FP (2012) Contributions of human enzymes in carcinogen metabolism. Chem Res Toxicol 25:1316–1383.
9. Sevrioukova IF, Poulos TL (2011) Structural biology of redox partner interactions in P450cam monooxygenase: a fresh look at an old system. Arch Biochem Biophys 507:66–74.
10. Katagiri M, Ganguli BN, Gunsalus IC (1968) A soluble cytochrome P-450 functional in methylene hydroxylation. J Biol Chem 243:3543–3546.
11. Kuznetsov VY, Poulos TL, Sevrioukova IF (2006) Putidaredoxin-to-cytochrome P450cam electron transfer: differences between the two reductive steps required for catalysis. Biochemistry 45:11934–11944.
12. Lipscomb JD, Sligar SG, Namtvedt MJ, Gunsalus IC (1976) Autooxidation and hydroxylation reactions of

oxygenated cytochrome P-450cam. J Biol Chem 251: 1116–1124.
13. Sevrioukova IF, Garcia C, Li H, Bhaskar B, Poulos TL (2003) Crystal structure of putidaredoxin, the [2Fe-2S] component of the P450cam monooxygenase system from *Pseudomonas putida*. J Mol Biol 333:377–392.
14. Sevrioukova IF, Li H, Poulos TL (2004) Crystal structure of putidaredoxin reductase from *Pseudomonas putida*, the final structural component of the cytochrome P450cam monooxygenase. J Mol Biol 336:889–902.
15. Sevrioukova IF, Poulos TL, Churbanova IY (2010) Crystal structure of the putidaredoxin reductase x putidaredoxin electron transfer complex. J Biol Chem 285:13616–13620.
16. Churbanova IY, Poulos TL, Sevrioukova IF (2010) Production and characterization of a functional putidaredoxin reductase-putidaredoxin covalent complex. Biochemistry 49:58–67.
17. Poulos TL, Finzel BC, Howard AJ (1987) High-resolution crystal structure of cytochrome P450cam. J Mol Biol 195:687–700.
18. Tripathi S, Li H, Poulos TL (2013) Structural basis for effector control and redox partner recognition in cytochrome P450. Science 340:1227–1230.
19. Hiruma Y, Hass MA, Kikui Y, Liu WM, Olmez B, Skinner SP, Blok A, Kloosterman A, Koteishi H, Lohr F, Schwalbe H, Nojiri M, Ubbink M (2013) The structure of the cytochrome p450cam-putidaredoxin complex determined by paramagnetic NMR spectroscopy and crystallography. J Mol Biol 425:4353–4365.
20. Pochapsky SS, Pochapsky TC, Wei JW (2003) A model for effector activity in a highly specific biological electron transfer complex: the cytochrome P450(cam)-putidaredoxin couple. Biochemistry 42:5649–5656.
21. Unno M, Christian JF, Benson DE, Gerber NC, Sligar SG, Champion PM (1997) Resonance Raman investigations of cytochrome P450(cam) complexed with putidaredoxin. J Am Chem Soc 119:6614–6620.
22. Myers WK, Lee YT, Britt RD, Goodin DB (2013) The conformation of P450cam in complex with putidaredoxin is dependent on oxidation state. J Am Chem Soc 135:11732–11735.
23. Nagano S, Shimada H, Tarumi A, Hishiki T, Kimata-Ariga Y, Egawa T, Suematsu M, Park SY, Adachi S, Shiro Y, Ishimura Y (2003) Infrared spectroscopic and mutational studies on putidaredoxin-induced conformational changes in ferrous CO-P450cam. Biochemistry 42:14507–14514.
24. Zhang W, Pochapsky SS, Pochapsky TC, Jain NU (2008) Solution NMR structure of putidaredoxin-cytochrome P450cam complex via a combined residual dipolar coupling-spin labeling approach suggests a role for Trp106 of putidaredoxin in complex formation. J Mol Biol 384:349–363.
25. Meharenna YT, Poulos TL (2010) Using molecular dynamics to probe the structural basis for enhanced stability in thermal stable cytochromes P450. Biochemistry 49:6680–6686.
26. Winn PJ, Ludemann SK, Gauges R, Lounnas V, Wade RC (2002) Comparison of the dynamics of substrate access channels in three cytochrome P450s reveals different opening mechanisms and a novel functional role for a buried arginine. Proc Natl Acad Sci USA 99: 5361–5366.
27. Koga H, Sagara Y, Yaoi T, Tsujimura M, Nakamura K, Sekimizu K, Makino R, Shimada H, Ishimura Y, Yura K, Co M, Ikeguchi M, Horiuchi T (1993) Essential role of the Arg112 residue of cytochrome P450cam for electron transfer from reduced putidaredoxin. FEBS Letts 331:109–113.
28. Nakamura K, Horiuchi T, Yasukochi T, Sekimizu K, Hara T, Sagara Y (1994) Significant contribution of arginine-112 and its positive charge of *Pseudomonas putida* cytochrome P-450cam in the electron transport from putidaredoxin. Biochim Biophys Acta 1207:40–48.
29. Sligar SG, Debrunner PG, Lipscomb JD, Namtvedt MJ, Gunsalus IC (1974) A role of the putidaredoxin COOH-terminus in P-450cam (cytochrome m) hydroxylations. Proc Natl Acad Sci USA 71:3906–3910.
30. Gerber NC, Sligar SG (1994) A role for Asp-251 in cytochrome P-450cam oxygen activation. J Biol Chem 269: 4260–4266.
31. Vidakovic M, Sligar SG, Li H, Poulos TL (1998) Understanding the role of the essential Asp251 in cytochrome p450cam using site-directed mutagenesis, crystallography, and kinetic solvent isotope effect. Biochemistry 37: 9211–9219.
32. Batabyal D, Poulos TL (2013) Crystal structures and functional characterization of wild-type CYP101D1 and its active site mutants. Biochemistry 52:8898–8906.
33. Case DA, Cheatham TE III, Darden T, Gohlke H, Luo R, Merz KM, Onufriev A, Simmerling C, Wang B, Woods RJ (2005) The Amber biomolecular simulation programs. J Comput Chem 26:1668–1688.
34. Shahrokh K, Orendt A, Yost GS, Cheatham TE III (2012) Quantum mechanically derived AMBER-compatible heme parameters for various states of the cytochrome P450 catalytic cycle. J Comput Chem 33: 119–133.
35. Wang J, Wolf RM, Caldwell JW, Kollman PA, Case DA (2004) Development and testing of a general amber force field. J Comput Chem 25:1157–1174.
36. Jakalian A, Bush BL, Jack DB, Bayly CI (2000) Fast, efficient generation of high-quality atom charges. AM1-BCC model: I. Method. J Comput Chem 21:132–146.
37. Jakalian A, Jack DB, Bayly CI (2002) Fast, efficient generation of high-quality atom charges. AM1-BCC model: II. Parameterization and validation. J Comput Chem 23:1623–1641.
38. Darden T, Perera L, Li L, Pedersen L (1999) New tricks for modelers from the crystallography toolkit: the particle mesh Ewald algorithm and its use in nucleic acid simulations. Structure 7:R55–R60.
39. Miyamoto S, Kollman PA (1992) SETTLE: an analytical version of the SHAKE and RATTLE algorithm for rigid water molecules. J Comput Chem 13:952–962.
40. Humphrey W, Dalke A, Schulten K (1996) VMD: visual molecular dynamics. J Mol Graphics 14:33–38.
41. Case DA, Cheatham TE III, Darden T, Gohlke H, Luo R, Merz KM Jr, Onufriev A, Simmerling C, Wang B, Woods RJ (2005) The Amber biomolecular simulation programs. J Comput Chem 26:1668–1688.